

Improved Torque and Efficiency of Induction Motors by Changing Rotor Structure of Permanent Magnet Assistance Synchronous Reluctance Motors

Bui Minh Dinh, Bui Duc Hung*, Trieu Viet Linh and Dang Quoc Vuong

School of Electrical and Electronic Engineering, Hanoi University of Science and Technology, Vietnam.

* Corresponding author. Email: hung.buiduc@hust.edu.vn

ARTICLE INFO

Received: 28/2/2022
Revised: 20/4/2022
Accepted: 25/4/2022
Published: 30/8/2022

KEYWORDS

Interior permanent magnet motor;
Electric vehicle;
Electromagnetic torque;
Electromagnetic field;
Finite element method.

ABSTRACT

Many authors have recently studied line start permanent magnet assistance synchronous reluctance. This paper presents a method to improve the electromagnetic torque and efficiency of induction motors of 7.5kW-4P (which consists of 36 stator slots and 40 rotor bars) by changing the design of the permanent magnet assistance synchronous reluctance rotors. This means that permanent magnets will be inserted into the squirrel cage induction motors (induction motors). The electromagnetic torque and efficiency of an induction motor are analyzed and compared with that of the line-start synchronous reluctance motor via a finite element analysis. In addition, the influence of position and length of permanent magnets on the electromagnetic torque and efficiency of the line-start synchronous reluctance motor is also considered and simulated. The model of this motor Linh is finally designed with four U layered- magnet rotors to verify the developed method. The development of the method is also validated by the practical induction motor.

Doi: <https://doi.org/10.54644/jte.71A.2022.1145>

Copyright © JTE. This is an open access article distributed under the terms and conditions of the [Creative Commons Attribution-NonCommercial 4.0 International License](https://creativecommons.org/licenses/by-nc/4.0/) which permits unrestricted use, distribution, and reproduction in any medium for non-commercial purpose, provided the original work is properly cited.

1. Introduction

The electric energy consumption of electric motors has been increasing in industrial applications up to 40% [1], [2]. For a low efficiency of the electric motor, environmental problems such as emission of greenhouse gases are created. In order to overcome these problems, the minimum energy performance standards (MEPS) are presented by changing the efficiency of motors. In practice, induction motors (IMs) account for 70% of industrial motors because of their low manufacturing cost and simple structure [3]. But, these motors appear copper losses leading to a limitation of the improvement in their efficiency [4]-[5]. Thus, in order to replace these motors, several types of motors are studied to improve the efficiency such as line-start synchronous reluctance motors (LS-SynRMs). For this motor, it can be operated at a synchronous speed without exhibiting secondary copper loss [5].

2. Finite Element approach

As presented in the previous part, so as to compare the efficiency of LS-SynRMs, the IM of and LS-SynRM with same power of 7.5 kW- 4P are designed as shown in Figure 1.

It should be noted that the main parameters of stators of two of these motors are the same, but the rotors are different. The number of squirrel cage bars of the reference motors is similar. Table 1 gives the diameter of stator and rotor, the air-gap length, the numbers of slot and poles, the air-gap length and stack length.

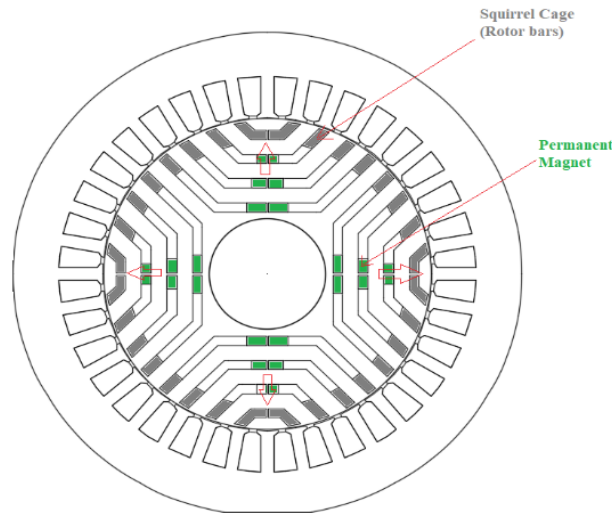


Figure 1. Model of LS-SynRM.

Table 1. Geometric parameters of LS-SynRM.

Parameters	Values	Unit
Slot number	36	
Outer Stator	210	mm
Inner Stator	132	mm
Slot Depth	19	mm
Tooth Width	5	mm
Magnet size	5x2	mm
Stator Lam Length	180	mm
Magnet Length	150	mm
Motor Length	180	mm
Air gap	0.4	mm
Turn per coil	20	

The geometric parameters of motor has been already calculated by estimation equations given in [1], [2]. An analytical model has been presented by many steps of computation to determine basic parameters. Based on a torque volume density (TVR) from 65 to 80 kNm/m³ [5], it is assumed that the rotor diameter (D) is equal to the rotor length (L), the electromagnetic torque (T) of the LS-SynRM can be thus defined as [6]-[8]

$$T = \frac{\pi}{4} \cdot D^2 \cdot L_s \cdot TRV, \quad (1)$$

where L_s is the length of core (m) and D is the out diameter (m).

In general, the LS-SynRM is designed in the same way of the IM. The main parameters (such as the rotor diameter, outer diameter, stator slot, motor length, and airgap length) can be determined as actual factors with the requirement of desired inputs.

3. Design of LS-SynRMs

The permanent magnet (PM) is embedded in rotor configuration of the LS-SynRM to create sufficiently the magnetic voltage for magnetic circuit. In practice, the possible configurations are classified by the shape and position of PMs mounted on the rotor as given in Table 1, such as the number

of poles, slots and stack lengths. The rotor topology of the proposed motor is presented in Figure 2. It can be also considered as the 4 layered-shape magnet arrangement.

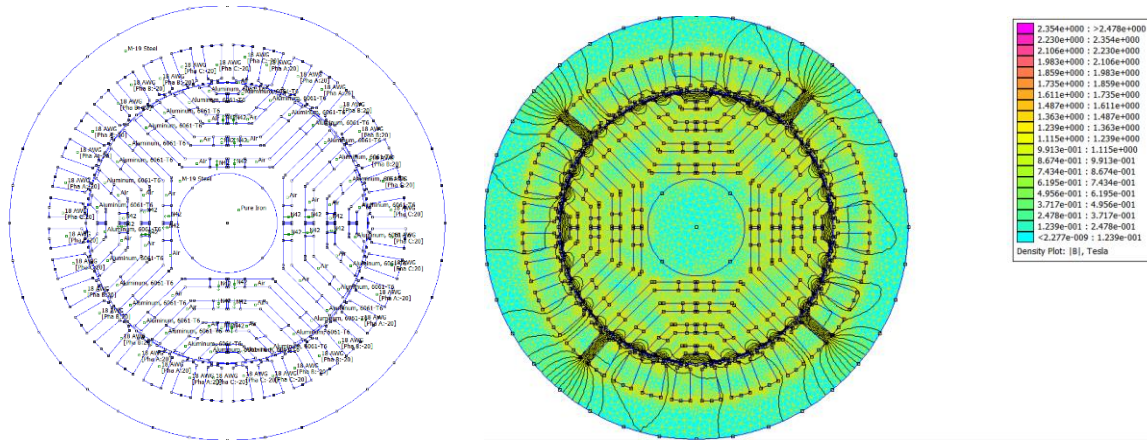


Figure 2. LS-SynRM with 4 layered magnets.

In practice, in order to obtain the maximum reluctance and electromagnetic torque, the number of PMs has to be limited. The PM arrangement is related to the efficient operation in the U-shape. The shapes of prototype model are very complicated to insert the PM inside the rotor. It is also very difficult to compare and combine the effectiveness of the PM position with all different sizes [9] - [11]. In general, the rib gives a fixed value based on the relation of manufacturing limitations. By coupling the Matlab program to CAD automatically program, the change in the number of flux barriers (K_w) can be expressed as

$$K_w = \frac{\sum W_{air}}{\sum W_{iron}}, \quad (2)$$

where $\sum W_{air}$ is the total flux barrier width and $\sum W_{iron}$ is the width of total rotor iron sheets. The total volumes of the PMs are pre-computed. It should be noted that the total weight of copper winding and magnet segment is the same. For one polar, the rotor structures consist of five and six pieces of magnets. Thus, it is very complicated. The geometric parameters of IP and LS- PMA-SYNRM are shown in Table 2.

Table 2. Geometric parameters of LS- PMA-SynRM

Parameter	IM (kg)	LS-PMA-SynRM (kg)
Stator Lam (Back Iron)	8.26	8.26
Stator Lam (Tooth)	5.245	5.245
Stator Lamination [Total]	13.5	13.5
Armature EWdg [Front]	1.027	1.027
Armature Winding [Active]	4.138	4.138
Armature EWdg [Rear]	1.027	1.027
Armature Winding [Total]	6.193	6.193
Wire Ins. [Total]	0.2172	0.2172
Rotor Lam (Back Iron)	5.248	5.37
Rot Inter Lam (Back Iron)	2.25E-05	2.25E-05
IPM Magnet Pole	4.723	4.833
Rotor Lamination [Total]	10.5	10.74
Magnet	-	0.5
Total	34.55	33.98

The back electromagnetic force (EMF) of 4U shape is the sinusoidal waveform. It gets a small value of 120V because the flux barriers are quite big and the magnet is considered as an assistance. The EMF of LS-PMA- SynRM is pointed out in Figure 3.

The main data of two models are given in Table 3, which consists of the average and ripple torque. The power losses, cogging torque and efficiency are then computed and simulated. It can be seen that the total losses due to the core loss and magnet eddy-current loss with four-segmented magnets are the lowest. Hence, this is a basic to select this model as the prototype machine.

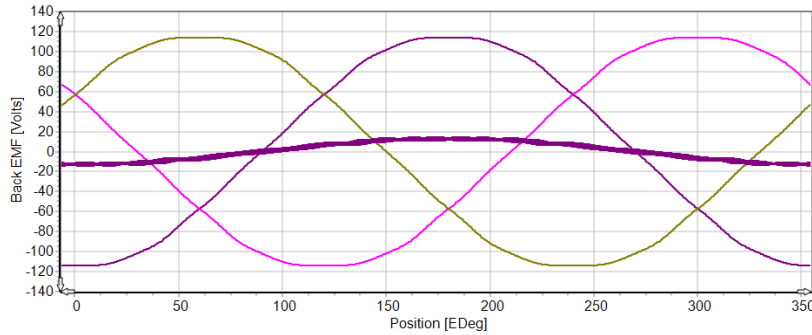


Figure 3. The back EMF of two models (SynRM and PMA-SynRM).

Table 3. Efficiency comparison of LS-PMA-SynRM and IM.

Parameter	LS-SynRM	IM	Unit
Shaft Torque	55.667	44.662	Nm
Input Power	9273.3	7597.5	Watts
Output Power	8744.1	7015.5	Watts
Total Losses (on load)	529.15	581.98	Watts
System Efficiency	94.294	92.34	%
Armature DC Copper Loss (on load)	340	382.7	Watts
Magnet Loss (on load)	178.8	188.5	Watts
Stator iron Loss [total] (on load)	10.33	10.78	Watts
Harmonic Distortion Line-Line Terminal Voltage	3.089	-	Volts
Phase Terminal Voltage (rms)	289.1	298.5	Volts
Harmonic Distortion Phase Terminal Voltage	11.27	-	%
Back EMF Line-Line Voltage (peak)	114	-	%
Back EMF Line-Line Voltage (rms)	82.29	-	Volts
Back EMF Phase Voltage (peak)	57.39	-	Volts

3.1. Performance Design

In this part, the model of PMA-SynRM motor is designed and compared with the IM model. The total torque and efficiency are important performance for those motors. The electromagnetic torque (T) of this motor is formed by the reluctance torque and magnetic torque. For the PM component, it is produced via the interaction between magnetic field at the airgap and the armature reaction magnetic field. For the reluctance component, it is replaced on the asymmetry between the magnetic circuit of d -axis and q -axis. Thus, the term T can be determined:

$$T = \frac{3 \cdot p}{2} [\lambda_{pm} \cdot i_d + (L_d - L_q) \cdot i_d \cdot i_q], \quad (3)$$

where p is the number of pole pairs, λ_{pm} is the linkage flux generated by the PM field, i_d , i_q are respectively direct and quadrature currents, and L_d , L_q are respectively direct and quadrature axis inductance. These parameters are calculated due to the rotor magnet barrier and magnet pole V angle.

The electromagnetic torque of reluctance and permanent magnetic parts are depicted in Figure 5. It presents that the 4U shape of PMA-SynRM motor gets a higher average torque of 10 $N.m$.

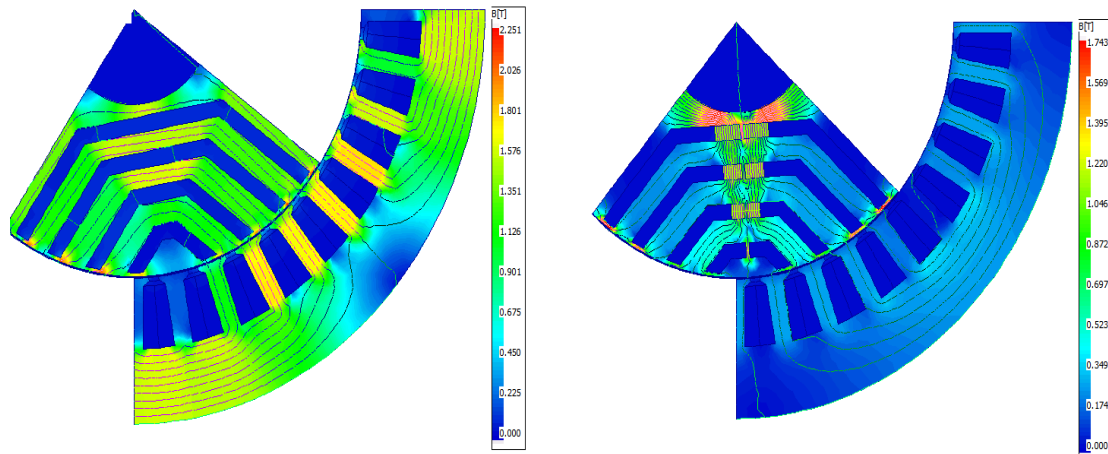


Figure 4. Flux density of reluctance (top) and Permanent Magnet Assistance (bottom).

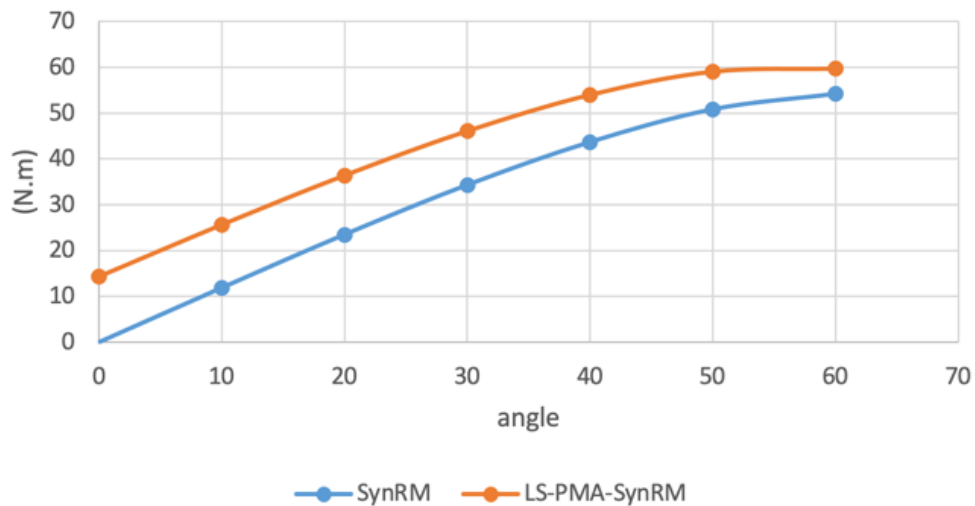


Figure 5. Comparison of ripple torque between 4U and 4V.

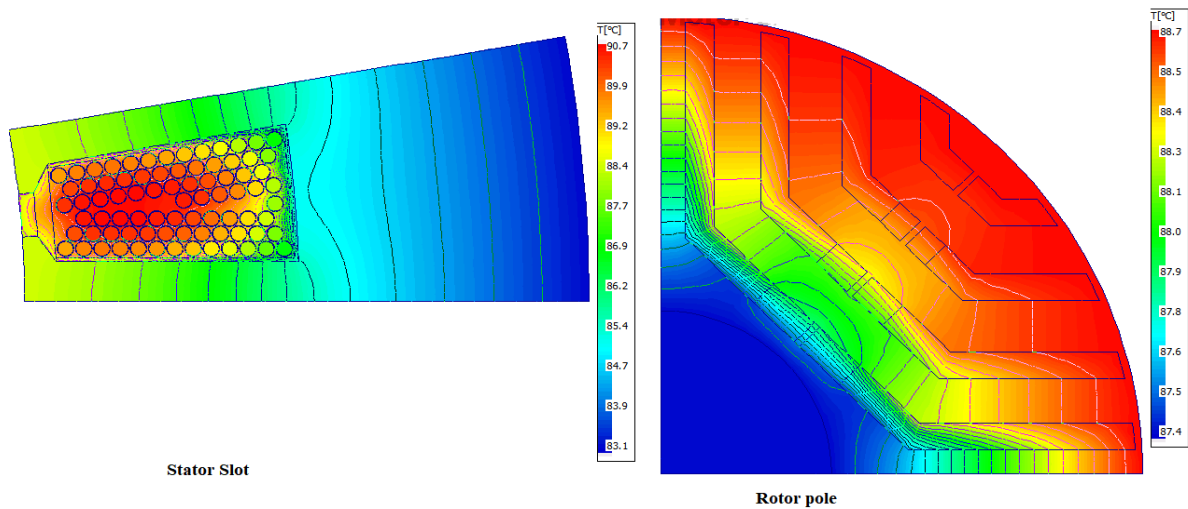


Figure 6. Temperature values of LS-PMa-SynRM

For the U shape of LS PMA-SynRM machine, the peak torque and power characteristics have been checked at 1500 rpm. The average torque is 52 Nm and the maximum efficiency is 94% for the phase current density of 5 A/mm². The iron and copper losses have been applied to the thermal simulation. Temperature results are presented in Figure 6 and Figure 7. The maximum temperature of winding is 90.7°C, which is lower than isolation class of H (180°C), and 88°C for the temperature of magnet. The detail values of other parts are given in Table 4.

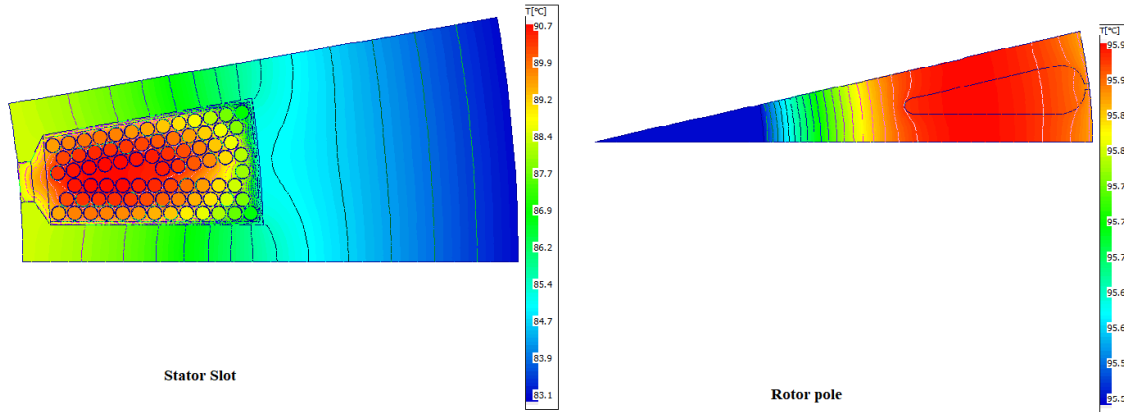


Figure 7. Temperature values of IM.

Table 4. Temperature of LS- PMA-SynRM and IM.

No	Component	LS-SynRM (T ⁰ C)	IM (T ⁰ C)
1	T [Ambient]	40	40
2	T [Housing - Active]	78.717	80.987
3	T [Stator Lam (back iron)]	84.833	83.33
4	T [Stator Surface]	88.403	86.24
5	T [Rotor Surface]	88.65	95.829
6	T [Airgap Banding]	88.651	95.992
7	T [Magnet]	88.197	--
8	T [Airgap Banding]	88.651	95.972
9	T [Rotor Lamination]	87.674	95.502
10	T [Shaft - Center]	87.375	88.422
13	T [Active Winding Minimum]	87.352	90.363

4. Conclusions

The model of four-layered LS PMA-SynRM motors with U-shape has been successfully proposed. It has been indicated that volume of magnets of the proposed structure is the lowest due to the closer air gap, high torque and power density. In addition, this type of shape gets the lower ripple torque and core loss, because the harmonics of air-gap density are reduced by the increase of magnet layers. In order to check the presented model, a detailed design of a three-phase hybrid rotor PM machine with 36 slots and 4 poles is proposed to verify the torque, power, and efficiency performances. The harmonic orders of the back electromotive force have been shown via the finite element analysis. The obtained results of temperatures from the thermal simulation have been also pointed out to validate the overheat capacity.

Acknowledgments

This research was supported by Institute for Control Engineering and Automation- ICEA for High Processing Speed Computer and CAD software to complete this paper.

REFERENCES

- [1] T. T.M. Do et al., "Evaluating online learning and teaching at the university of Technology and Education Ho Chi Minh City during Coronavirus pandemic," *Journal of Technical Education Science*, no. 62, pp. 17–27, Feb. 2021. DOI: 10.54644/jte62202158
- [2] G. O. Young, "Synthetic structure of industrial plastics," in *Plastics*, 2nd ed., vol. 3, J. Peters, Ed., New York, NY, USA: McGraw-Hill, 1964, pp. 15–64.
- [3] H. Kim, Y. Park, S.-T. Oh, H. Jang, D.-H. Jung, I. S. Jang, and J. Lee, "Study on Analysis Method of Asymmetric Permanent Magnet Assistance Synchronous Reluctance Motor Considering Magnetic Neutral Plane Shift," *IEEE Transactions on Applied Superconductivity Year*, Vol.30, no. 4, 2020.
- [4] B. Ozpineci, "Oak Ridge National Laboratory annual progress report for the electric drive technologies program," Oak Ridge Nat. Lab., Oak Ridge, TN, USA, Tech. Rep. ORNL/SR-2016/640, Oct. 2016.
- [5] X. Chen, J. Wang, B. Sen, P. Lazari, and T. Sun, "A high-fidelity and computationally efficient model for interior permanent-magnet machines considering the magnetic saturation, spatial harmonics, and iron loss effect," *IEEE Trans. Ind. Electron.*, vol. 62, no. 7, pp. 4044–4055, Jul. 2015.
- [6] C. Gong and F. Deng, "Design and Optimization of a Low-Torque-Ripple High-Torque-Density Vernier Machine Using Ferrite Magnets for Low-Speed Direct-Drive Applications" *2021 IEEE International Electric Machines & Drives Conference (IEMDC)*, 2021.
- [7] M. Taniguchi et al., "Development of new hybrid transaxle for compact class vehicles," *SAE Tech.*, Paper 2016-01-1163, 2016, doi: 10.4271/2016-01-1163.
- [8] T. Huynh and M.-F. Hsieh, "Comparative study of PM-assisted SynRM and PMA-SYNRMSM on constant power speed range for EV applications," *IEEE Trans. Magn.*, vol. 53, no. 11, Art. no. 8211006, Nov. 2017.
- [9] S. Zhu, W. Chen, M. Xie, C. Liu and K. Wang, "Electromagnetic Performance Comparison of Multi-Layered Interior Permanent Magnet Machines for EV Traction Applications," in *IEEE Transactions on Magnetics*, vol.54, no.11, pp.1-5, Art no.8104805, Nov.2018, doi: 10.1109/TMAG.2018.2841851.
- [10] Y. Nie, I. P. Brown, and D. C. Ludois, "Deadbeat-direct torque and flux control for wound field synchronous machines," *IEEE Trans. Ind. Electron.*, vol. 65, no. 3, pp. 2069–2079, Mar. 2018.
- [11] A. Wang, Y. Jia, and W. L. Soong, "Comparison of five topologies for an interior permanent-magnet machine for a hybrid electric vehicle," *IEEE Trans. Magn.*, vol. 47, no 10, pp. 3606-3609, Oct. 2011.



Dr. Bui Minh Dinh is currently working as a lecturer at Department of Electrical Engineering, School of Electrical and Electronic Engineering, Hanoi University of Science and Technology. He obtained the PhD degree in the Department of Electrical Engineering, TU university, in 2014.



Dr. Bui Duc Hung is currently working as a team leader of electrical machines's group, and also a lecturer of Department of Electrical Engineering, School of Electrical Engineering, Hanoi University of Science and Technology. He obtained the PhD degree in the Department of Electrical Engineering, Hanoi University of Science and Technology, in 2000.



Dr. Trieu Viet Linh is currently working as a lecturer of electrical machines's group, and also a lecturer of Department of Electrical Engineering, School of Electrical Engineering, Hanoi University of Science and Technology. He obtained the PhD degree in the Department of Electrical Engineering, Hanoi University of Science and Technology, in 1999.



Assoc. Prof. Dang Quoc Vuong is currently a deputy director of Training Center of Electrical and Electronic Engineering, and also a lecturer of Department of Electrical Engineering, School of Electrical Engineering, Hanoi University of Science and Technology. He obtained the PhD degree in the Electrical Engineering and Computer Science Department of the University of Liège, Belgium, in 2013.